Received: 4 October 2022 | Accepted: 17 October 2022

DOI: 10.1002/pamm.202200076

Modelling and simulation of time-dependent damage and failure within silicone-based, polymeric adhesives

Lukas Lamm[1,*], **Jan Mirco Pfeifer**[1,2], **Hagen Holthusen**[1], **Tim Brepols**[1], and **Stefanie Reese**[1]

[1] Institute of Applied Mechanics, RWTH Aachen University, Mies-van-der-Rohe-Str. 1, 52074 Aachen, Germany
[2] Baumechanik und Numerische Methoden, University of Wuppertal, Pauluskirchstr. 7, 42285 Wuppertal, Germany

Hyperelastic adhesive joints are used successfully in many areas of industry. Besides all their inherent advantages, materials used for the construction of such bonds show a vast variety of non-linear effects in their response to mechanical loading, which poses a challenge in modelling and predicting their material response. Recent experiments have shown a strong temporal response when it comes to damage and failure within these materials. This contribution aims to propose a simple but yet flexible formulation to predict time-dependent damage effects within polymeric adhesives. Besides the main aspects of the thermodynamically consistent development, we also show numerical examples to demonstrate the capabilities of the model.

1 Introduction

Adhesives are widely used in the industrial context. Especially in the building industry, their use in the construction of glass façade systems is becoming increasingly important [1]. To ensure safe application, the material behaviour under real load conditions must be predicted with high accuracy. Computational models have proven their worth for this purpose. In addition to the highly non-linear elastic material behaviour, such models must also be able to represent a wide range of inelastic, temperature-dependent and rate-dependent effects. Just recently [2] and [3] found that such adhesives do show a pronounced time-dependent behaviour when it comes to damage and failure. These effects can not be described by a classical rate-independent viscoelastic damage model. Modelling time-dependent inelastic behaviour of solids is nothing new. In the field of damage modelling, however, approaches are often used which assume small deformations. The so called *creep damage model* developed by [4] and later modified by [5] lays the ground for a variety of models used e.g. in the modelling of damage in rock or asphalt (see e.g. [6], [7] or [8]). Further approaches using *viscous regularization* as described in the work of [9] are e.g. [10], [11] or [12]. The assumption of small deformations can no longer be assumed to be true for hyperelastic adhesives. Within this contribution we therefore follow an approach similar to *viscous regularization* but extend it to describe material responses at finite strains. The model proposed is simple yet powerful for modelling time-dependent isotropic damage. To study the effects of this modelling approach, we solely focus on this single type of temporal inelastic effect. For this, we derive a thermodynamically consistent material formulation based on the gradient extended micromorphic framework of [13] and extend it with a Perzyna-type ansatz [9, 14] to capture the temporal effects. We also show the algorithmic implementation strategy as well as selected numerical examples to evaluate the capabilities of the given model.

2 Continuum mechanical modelling

As frequently done within the modelling of hyperelastic polymeric materials, we start with the well-established multiplicative split of the deformation gradient $\mathbf{F}$ into volumetric and isochoric parts (see e.g. [15, 16]), i.e.

$$\mathbf{F} = \det \mathbf{F}^{\frac{1}{3}} \mathbf{I} \mathbf{F}^{*} = J^{\frac{1}{3}} \mathbf{F}^{*}. \tag{1}$$

With this at hand, the isochoric right Cauchy-Green tensor can be defined as $\mathbf{C}^{*} = J^{-\frac{2}{3}} \mathbf{F}^{T} \mathbf{F}$. To describe the damage behaviour within hyperelastic polymeric adhesives an isotropic evolution of damage within the material is assumed. Therefore, a scalar damage variable $D \in [0, 1]$ can be defined. The state of this variable determines the amount of accumulated damage. In this context, $D = 0$ describes the undamaged, virgin material whereas $D = 1$ means total failure of the material. Since the focus of this work is the investigation of time-dependent damage phenomena within polymeric adhesives, we assume the underlying basic material response to be hyperelastic. It is obvious that this is a strong assumption since polymers tend to show a pronounced time-dependent material response even within the purely elastic loading regime. For the sake of investigating the effects of time-dependent damage, it seems beneficial to isolate this modelling approach from further temporal dependencies and focus merely on the effects shown by the damage model itself. Therefore, the Helmholtz free energy can be defined by means of a damage degradation function $f_d(D) = (1 - D)^2$ such that

$$\psi := f_d(D) \psi_e(J, \mathbf{C}^{*}) + \psi_d(\xi_d) + \psi_{\bar{d}}(D, \bar{D}, \nabla \bar{D}). \tag{2}$$

* Corresponding author: e-mail lukas.lamm@ifam.rwth-aachen.de, phone +49 241 80 25006, fax +49 241 80 22001

Here, ψ_e is the elastically stored strain energy which is defined in terms of the symmetric right Cauchy-Green tensor $\mathbf{C} = \mathbf{F}^T\mathbf{F}$ with $\mathbf{F}$ being the deformation gradient. To describe damage hardening, we furthermore introduce the hardening variable ξ_d as well as the associated hardening energy ψ_d. It is well known that classical damage models tend to show pathological mesh dependencies accompanied by strong localization effects [17]. To avoid such effects, we make use of a gradient-extended ansatz as proposed by [13]. For this, the global damage variable $\bar{D}$ is introduced together with its associated free energy $\psi_{\bar{d}}$.

2.1 Thermodynamic considerations

In order to ensure physical correctness of the developed material model, the second law of thermodynamics must be fulfilled. Taking the given micromorphic extension into account it can be written in terms of the isothermal Clausius-Duhem inequality as

$$\mathbf{S} : \frac{1}{2}\dot{\mathbf{C}} - \dot{\psi} + \underbrace{a\dot{\bar{D}} + \mathbf{b} \cdot \nabla\dot{\bar{D}}}_{\text{micromorphic ext.}} \geq 0. \tag{3}$$

Here, $\mathbf{S}$ denotes the second Piola-Kirchhoff stress tensor whereas a and $\mathbf{b}$ describe the generalized stresses related to the non-local variable $\bar{D}$ and its gradient, respectively. For a more detailed elaboration the interested reader is kindly referred to [18]. Inserting Equation (2) into Equation (3) and applying the standard Coleman-Noll procedure [19] yields the thermodynamically consistent definition of the second Piola-Kirchhoff stress tensor

$$\mathbf{S} = 2f_d \frac{\partial \psi_e}{\partial \mathbf{C}} \tag{4}$$

together with the generalized stresses $a = \frac{\partial \psi_{\bar{d}}}{\partial \bar{D}}$ and $\mathbf{b} = \frac{\partial \psi_{\bar{d}}}{\partial \nabla \bar{D}}$. Defining the thermodynamically conjugated driving forces for the damage variable D as well as the damage hardening variable ξ_d as $Y = -(\frac{\partial f_d}{\partial D}\psi_e + \frac{\partial \psi_{\bar{d}}}{\partial D})$ and $q_d = \frac{\partial \psi_d}{\partial \xi_d}$ leads to the reduced Clausius-Duhem inequality given by

$$Y\dot{D} - q_d\dot{\xi}_d \geq 0. \tag{5}$$

In order to ensure thermodynamical consistency, evolution equations for D and ξ_d must be found that fulfil this reduced inequality.

2.2 Evolution equations

In order to describe the onset of damage evolution within the material, we follow the standard approach of defining a scalar damage function as

$$\Phi_d = Y - (Y_0 + q_d), \tag{6}$$

which includes the damage threshold parameter Y_0. Next, we introduce the so-called damage multiplier $\dot{\lambda}_d$ and postulate an associative evolution law for both, the damage variable D as well as the hardening variable ξ_d, i.e.

$$\dot{D} = \dot{\lambda}_d \frac{\partial \Phi_d}{\partial Y} = \dot{\lambda}_d \qquad \text{and} \qquad \dot{\xi}_d = -\dot{\lambda}_d \frac{\partial \Phi_d}{\partial q_d} = \dot{\lambda}_d. \tag{7}$$

This particular choice of the evolution equations has the effect that the evolution of D and ξ_d are equivalent. It is important to notice that this is a rather simple assumption and by no means the only possible definition of associative evolution laws for D or ξ_d. For classical rate-independent isotropic damage, the definition of Equations (6) and (7) is sufficient and could be solved using Karush-Kuhn-Tucker conditions.

To introduce a temporal dependency into the damage model at hand, we adapt an ansatz made by e.g. [9, 14] or [20] where we explicitly define an extra evolution equation for the damage multiplier $\dot{\lambda}_d$ such that

$$\dot{\lambda}_d = \begin{cases} \eta_d \, \Phi_d^{\frac{1}{\epsilon_d}} & \text{if} \quad \Phi_d \geq 0 \\ 0 & \text{if} \quad \Phi_d < 0 \end{cases} \tag{8}$$

Here, η_d describes a damage velocity and ϵ_d is the damage rate sensitivity.

2.3 Particular choice of the Helmhotz free energies

Depending on the material at hand, various hyperelastic ground models are applicable. For hyperelastic polymers which are showing pronounced strain-stiffening effects models such as [21] or [22] seem to be a good choice. Since the focus of this

study is merely the time-dependent damage behaviour and for the sake of simplicity, we make use of a classical Neo-Hookean type energy to describe the underlying elastic material response, i.e.

$$\psi_e(J, \mathbf{C}^*) := \frac{\mu}{2}\left(\operatorname{tr}\mathbf{C}^* - 3\right) + \frac{\kappa}{4}\left(J^2 - 1 - 2\ln J\right). \tag{9}$$

To describe the energy density associated with damage hardening, a combination of linear and nonlinear, Voce-type hardening [23] is used, i.e.

$$\psi_d(\xi_d) := \underbrace{\frac{1}{2}\,k\,\xi_d^2}_{\text{lin. hardening}} + \underbrace{r\left(\xi_d + \frac{1}{s}\left[\exp(-s\xi_d) - 1\right]\right)}_{\text{Voce-type hardening}}. \tag{10}$$

Here, r, s and k are material parameters controlling the damage hardening behaviour. Regarding the energy density of the mircormorphic gradient extension, we define $\psi_{\bar{d}}$ in accordance with [18] as

$$\psi_{\bar{d}}(D, \bar{D}, \nabla\bar{D}) := \frac{H}{2}\left(D - \bar{D}\right)^2 + \frac{A}{2}\nabla\bar{D}\cdot\nabla\bar{D}, \tag{11}$$

where the parameters H and A describe the coupling between local and non-local damage fields as well as the influence of the gradient of $\bar{D}$.

These choices of the individual parts of the Helmholtz free energy yield for the thermodynamically conjugated driving forces the following expressions:

$$Y = -\left(2(1-D)\psi_e + H(D - \bar{D})\right) \qquad \text{and} \qquad q_d = k\,\xi_d + r - \exp(-s\xi_d) \tag{12}$$

3 Algorithmic implementation

The material formulation described above has been implemented into the multipurpose finite element program *FEAP*. For the solution of evolution Equation (7) together with Equation (8) we apply an implicit Euler integration scheme with time step size $\Delta t = t_{n+1} - t_n$, such that

$$r = D_{n+1} - D_n - \eta_d\,\Phi_d^{\frac{1}{\epsilon_d}}\,\Delta t \stackrel{!}{=} 0. \tag{13}$$

This non-linear residual equation can be solved using standard Newton-Raphson iteration, for which the local tangent operator $\frac{\partial r}{\partial D}$ must be computed. Within this contribution, we used the automatic differentiation framework *AceGen* (see [24, 25]) to obtain this derivative. With this at hand the current value of the local damage variable D can be iteratively determined for the kth iteration step via $D_{k+1} = D_k - \frac{\partial r}{\partial D}^{-1} r_k$.

The local material response is implicitly included within the global material tangent operator of the finite element simulation. We therefore need to derive this tangent in a consistent manner in order to achieve quadratic convergence of the global iteration scheme. Since the second Piola-Kirchhoff stress tensor is a function of the right Cauchy-Green tensor as well as the internal variables, the tangent operator can be expressed as

$$\mathbb{C} = 2\left(\left.\frac{\partial\mathbf{S}}{\partial\mathbf{C}}\right|_D + \left.\frac{\partial\mathbf{S}}{\partial D}\right|_{\mathbf{C}} : \frac{\partial D}{\partial\mathbf{C}}\right). \tag{14}$$

For the given choices of the Helmholtz free energies from the last section, the partial derivative of the second Piola-Kirchhoff stress tensor with respect to the right Cauchy-Green tensor can be computed easily using *AceGen*. For the partial derivative of the local damage variable D with respect to the right Cauchy-Green tensor $\mathbf{C}$ we make use of the relation

$$\Delta D = \frac{\partial D}{\partial\mathbf{C}}\Delta\mathbf{C} = -\frac{\partial r}{\partial D}^{-1}\frac{\partial r}{\partial\mathbf{C}}\Delta\mathbf{C}, \tag{15}$$

where we use the fully converged residual and jacobian from the local solution process.

4 Numerical examples

In the following, we demonstrate the behaviour of the model described above showing some numerical studies conducted at integration point level. For this, a uniaxial loading state is applied whilst the damage associated material parameters are varied. For the elastic parameters we choose the shear modulus to be $\mu = 6.0$ MPa whilst the bulk modulus is set to $\kappa = 10000\mu$ which enforces nearly incompressible material behaviour. In order to avoid locking effects, we adapted a reduced integration finite element formulation with adaptive hourglass stabilization as described in [26].

4.1 Linear displacement simulation

The first example given in Figure 1 shows the results from a uniaxially loaded single element simulation over time. Here, a displacement $u(t)$ is applied at a constant rate $\frac{\mathrm{d}u}{\mathrm{d}t}$. Figures 1a and 1b clearly show the pronounced time dependency of the damage response with respect to time. For small values of the relaxation velocity η_d the model shows nearly no damage at all resulting in a response similar to classical Neo-Hookean elasticity. In case of high values of η_d we observe results similar to what is expected from a rate-independent model. Values of η_d in between these two edge case are able to interpolate the time-dependency nicely.

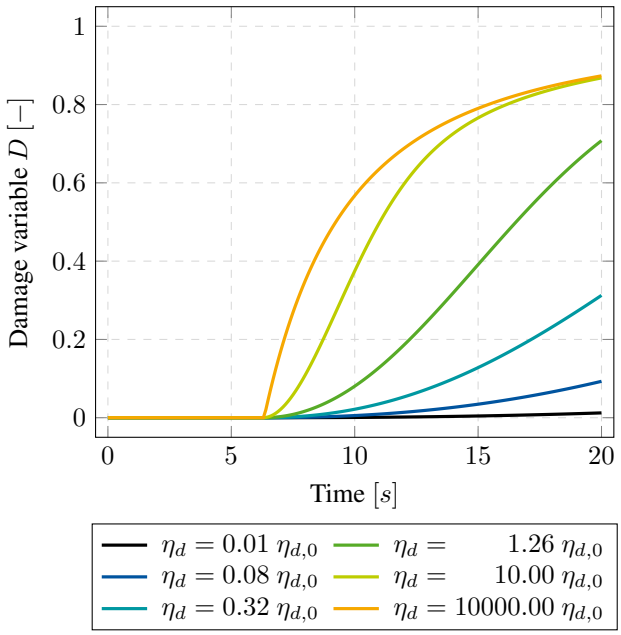

(a) Evolution of damage variable D.

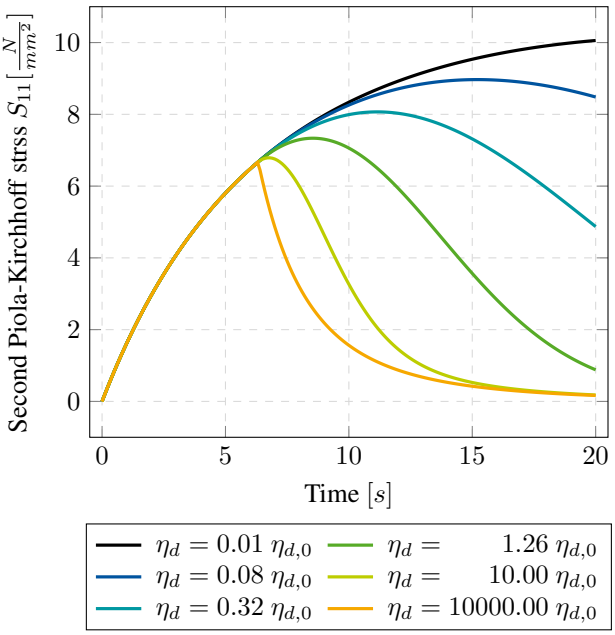

(b) Evolution of sec. Piola-Kirchhoff stress S_{11} in loading direction.

Fig. 1: Results of linear displacement applied uniaxially to a single element. Showing the influence of the damage relaxation velocity η_d with reference $\eta_{d,0} = 10^{-2}$. Reaction force normalized wrt. $F_{max} = 20.25$ N.

*

4.2 Relaxation simulation

The next example considers a classical relaxation simulation where a constant displacement $u(t)$ is applied at time $t = 1$s and held constant for the remainder of the simulation. Figure 2 shows the influence of both, the relaxation velocity η_d as well as the damage threshold Y_0. As already discussed in the previous example, the relaxation velocity as shown in Figure 2a is able to produces smooth interpolations between the pure elastic response for small values of η_d and the nearly rate-independent damage response for large values. Figure 2b shows the influence of Y_0 on the damage progression. Here it is obvious that smaller values lead to a more pronounced damage behaviour whereas larger values result in a more subtle damage progression and consequently in a higher residual reaction force. This behaviour is as expected, since the damage related driving force Y decreases with increasing damage progression and consequently falls below Y_0 faster for

4.3 Creep simulation

In the last example, we take a closer look at a classical creep simulation setup. For this, a constant force F_x is applied uniaxially at time $t = 1s$ and held constant over the rest of the simulation. Figure 3 shows the influence of the damage relaxation time η_d as well as of the damage threshold Y_0. Both evaluations shown in Figures 3a and 3b show the expected damage behaviour.

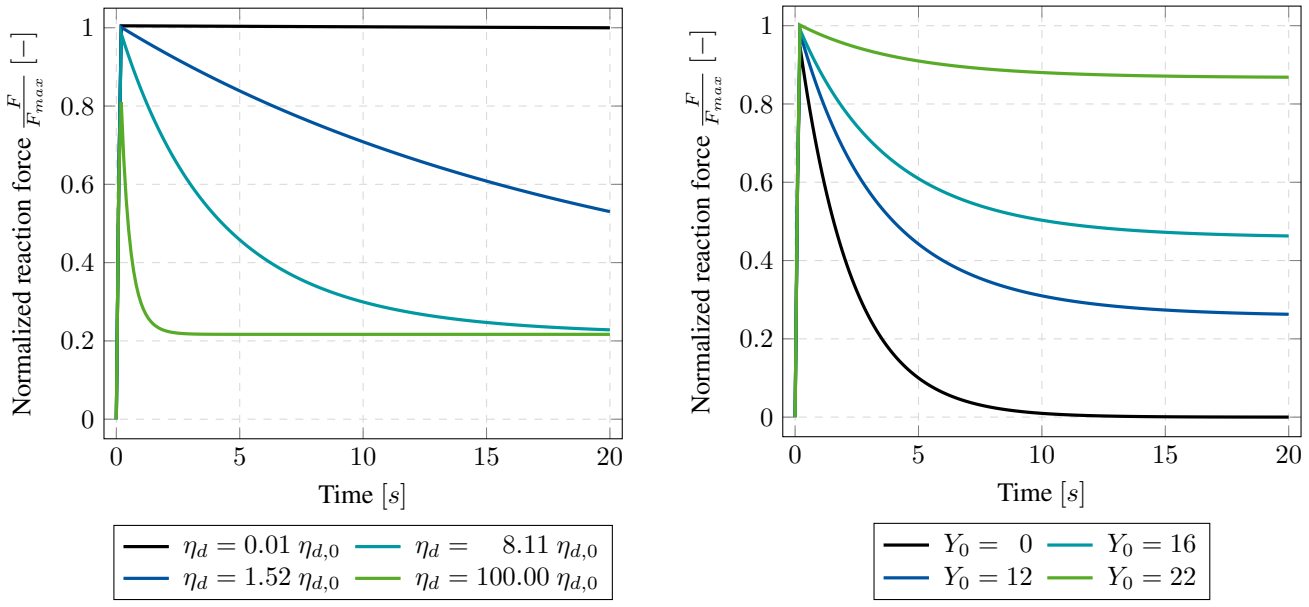

(a) Influence of damage relaxation velocity η_d.

(b) Influence of damage threshold Y_0.

Fig. 2: Results of relaxation experiment applied uniaxially to a single element. Showing the influence of material parameters η_d and Y_0 with reference $\eta_{d,0} = 10^{-3}$. Reaction force normalized wrt. $F_{max} = 20.25$ N.

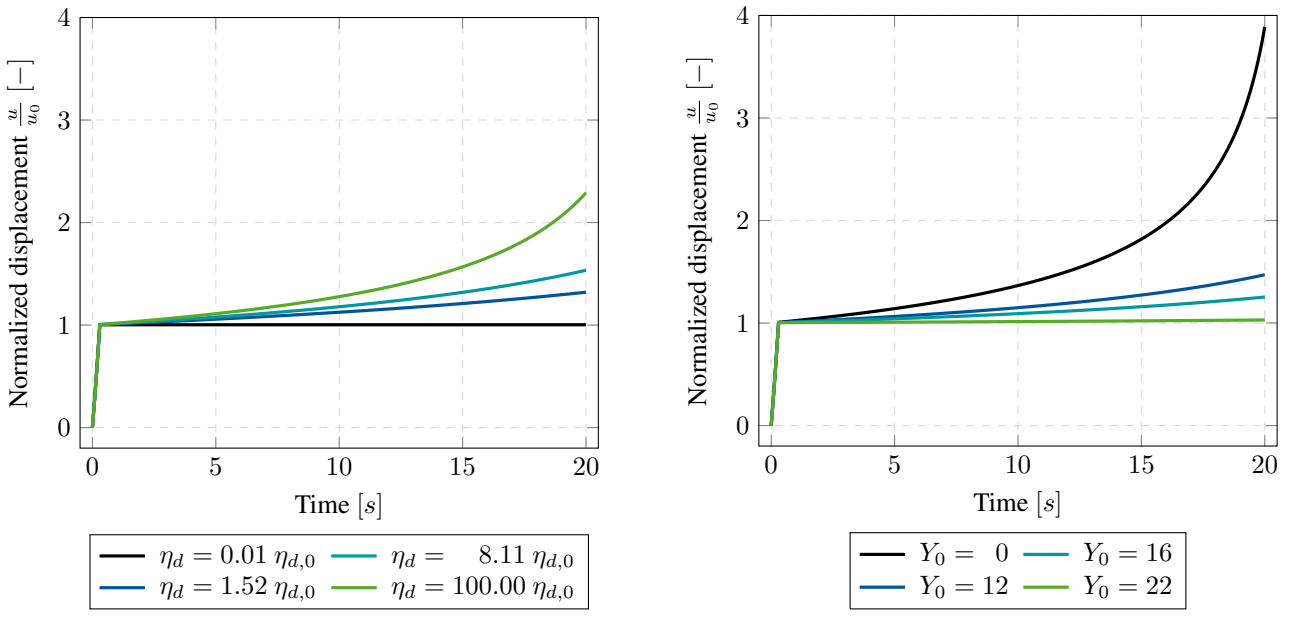

(a) Influence of damage relaxation velocity η_d.

(b) Influence of damage threshold Y_0.

Fig. 3: Results of creep experiment applied uniaxially to a single element. Showing the influence of material parameters η_d and Y_0 with reference $\eta_{d,0} = 10^{-3}$. Displacement normalized wrt. $u_0 = 0.125$ mm.

For small relaxation velocities η_d, the quasi-elastic response is achieved, whereas for large η_d an exponential growth in the displacement can be measured. This effect is even more pronounced when looking at the influence of the damage threshold Y_0. Since this measure describes the amount of energy that must be present in order to trigger damage effects, lower values of Y_0 lead to a faster and more pronounced damage progression. a higher threshold.

5 Conclusion and outlook

In this work, we have presented a simple yet felxible approach to modelling rate-dependent isotropic damage at finite deformation. To account for the temporal dependence of the material, we used a Perzyna-type approach to describe the evolution equations of damage. With this at hand, we were able to briefly demonstrate the reasonability of the material response for three different use-cases. Besides uniaxial linear deformation, also relaxation and creep simulations were shown. From a qualitative point of view, these studies gave reasonable results. Nevertheless, the model must still be validated using experimental data. Unfortunately, time-dependent damage is usually not observed as an isolated effect in real world materials but rather coupled with other inelastic effects, such as viscoelasticity in polymeric materials. Therefore, an extension of the given model to capture also viscoelasticity must be done before proceeding with the experimental validation of the model. Since polymers are known for their strongly temperature-dependent material behaviour, an extension of the model into a thermomechanically coupled formulation seems reasonable.

Acknowledgements Financial support by the *Arbeitsgemeinschaft industrieller Forschungsvereinigungen „Otto von Guericke“ e.V.* (AiF) through the project grant IGF 21348 N/3 is gratefully acknowledged. We furthermore gratefully acknowledge the financial support provided by the *German Research Foundation* (DFG) through the projects RE 1057/45-1 (No. 403471716) and RE 1057/46-1 (No. 404502442). Open access funding enabled and organized by Projekt DEAL.

References

[1] J. Klosowski, A. T. Wolf, Sealants in Construction 2nd Edition (CRC Press, Boca Raton, 2015), p. 1 - 20.
[2] R. Seewald, M. A. Schnittcher et al., International Journal of Adhesion and Adhesives **117**, 103016 (2021)
[3] B. Schaaf, M. Feldmann et al., ce/papers **5**, 87 - 100 (2022)
[4] L. Kachanov, Otdelenie Teckhnicheskikh Nauk **8**, 26 - 31 (1958)
[5] N. Rabotnov, Applied Mechanics, 342 - 349 (1969)
[6] M. G. Geers, W. A. M. Brekelmans, R. de Borst, DIANA Computational Mechanics **94**, 127 - 138 (1994)
[7] R. Wang, W. Xu, W. Wang, J. Zhang, European Journal of Environmental and Civil Engineering **17**, 111 - 125 (2013)
[8] G.-W. Zeng, X.-H. Yang, F. Bai, H. Gao, Journal of Central South University **21**, 4007 - 4013 (2014)
[9] P. Perzyna, Quarterly of Applied Mathematics **20**, 321-332 (1963)
[10] J.C. Simo, J. W. Ju, International Journal of Solids and Structures **23**, 821 - 840 (1987)
[11] M. Cervera, J. Oliver, O. Manzoli, Earthquake Engineering & Structural Dynamics **25**, 987 - 1010 (1996)
[12] X. Ren, J. Li, International Journal of Damage Mechanics **22**, 530 - 555 (2013)
[13] T. Brepols, S. Wulfinghoff, S. Reese, International Journal of Plasticity **129**, 102635 (2020)
[14] P. Perzyna, Advances of Applied Mechanics, 243-377 (1966)
[15] J. Lubliner, Mechanics Research Communications **12**, 93-99 (1985)
[16] J. C. Simo, R. L. Taylor, Computer Methods in Applied Mechanics and Engineering **85**, 273-310 (1991)
[17] E. Rizzi, I. Carol, K. Willam, Journal of Engineering Mechanics **121**, 541 - 554 (1996)
[18] S. Forest, Journal of Engineering Mechanics **135**, (2009)
[19] B. D. Coleman, W. Noll, Archive for Rational Mechanics and Analysis **13**, 1432-1673 (1963)
[20] D. Perić, International Journal for Numerical Methods in Engineering **36**, 1365-1393 (1993)
[21] E. M. Arruda, M. C. Boyce, Journal of the Mechanics and Physics of Solids **41**, 389-412 (1993)
[22] R. W. Ogden, Proceeding of the Royal Society London A **326**, 565-584 (1972)
[23] E. Voce, Journal of the Institute of Metals **74**, 537-562 (1948)
[24] J. Korelc, Engineering with Computers **18**, 312-327 (2002)
[25] J. Korelc, Computational Mechanics **44**, 631 - 649 (2009)
[26] O. Barfusz, T. Brepols et al., Computer Methods in Applied Mechanics and Engineering **373**, 113440 (2021)

